Journal of Alloys and Compounds 509 (2011) L95–L98

Contents lists available at ScienceDirect

Journal of Alloys and Compounds

journal homepage: www.elsevier.com/locate/jallcom

Letter

Fabrication and characterization of ceramic thin films by RF magnetron sputtering using Zn-enriched $(Ba_{0.3}Sr_{0.7})(Zn_{1/3}Nb_{2/3})O_3$ as target

Feifei Ji, Feng Shi*

College of Physics and Electronics, Shandong Normal University, No. 88th, East Wenhua Road, Jinan, 250014, PR China

ARTICLE INFO

Article history:
Received 8 October 2010
Received in revised form
22 November 2010
Accepted 23 November 2010
Available online 30 November 2010

Keywords:
Ceramic thin films
Crystal growth
Scanning and transmission electron microscope
X-ray scattering
Sputtering deposition

ABSTRACT

Dielectric ceramic thin film was fabricated on SiO_2 (1 1 0) substrates by radio frequency (RF) magnetron sputtering method using a Zn-enriched $(Ba_{0.3}Sr_{0.7})(Zn_{1/3}Nb_{2/3})O_3$ target. The microstructure, components, and morphological properties of the thin films were characterized thoroughly. The results reveal that the main phases of the thin films are $Ba_xSr_{1-x}Nb_2O_6$, which are of different compositions from that of the ceramic target due to Zn loss. The thin films are polycrystalline and of dense structure with uniform grain sizes and well-defined grain boundaries.

1. Introduction

Recently, dielectric ceramic thin films have been intensively studied for the potential applications in microelectronic and microwave integration circuits [1,2]. The researches of these ceramic thin films, such as $Ba(Zr_{0.3}Ti_{0.7})O_3$ [3], $BaTi_4O_9$ [4], and $Ba(Zn_{1/3}Ta_{2/3})O_3$ [2] have been reported by different methods such as Sol–Gel [5], PLD [2], and so on. In the past years, our group has studied ceramic thin films fabricated by radio frequency (RF) magnetron sputtering method using stoichiometric $(Ba_{0.3}Sr_{0.7})(Zn_{1/3}Nb_{2/3})O_3$ ceramic as target [6,7]. However, there exist many problems for these thin films, such as the composition discrepancy between the target and the thin films (i.e., serious Zn-loss) and oxygen-vacancies not only in PLD method [2] but also in magnetron sputtering deposition [3,4,6,7]. Taking into account that a major barrier in the widespread use of these films in a number of high-frequency applications is their high leakage currents determined by structural defects as grain boundaries and oxygen vacancies [8], it is significant for the research on the microstructure and the composition of the thin films. To obtain a dense thin film with fewer oxygen vacancies and less Zn loss, in this article, we adjusted the target component to fabricate ceramic thin films using magnetron sputtering deposition, which differs from those targets reported previously [6,7], i.e., 1 mol excess ZnO was incorporate in this stoichiometric $(Ba_{0.3}Sr_{0.7})(Zn_{1/3}Nb_{2/3})O_3$ target so as to compensate the ZnO volatilization during the sputtering and annealing process.

2. Experimental procedure

Ceramic thin films were deposited on SiO_2 (1 1 0) substrates by RF magnetron sputtering, using a Zn-enriched target comprised of a homogeneous mixture of 1 mol $(Ba_{0.3}Sr_{0.7})(Zn_{1/3}Nb_{2/3})O_3$ and 1 mol ZnO, which were synthesized by a conventional solid-state sintering technique. The monocrystal SiO_2 (1 1 0) substrates were placed on the substrate holder, which can rotate around a central axis to improve the homogeneity of the thin films. The thin films were deposited using an $Ar–O_2$ gas mixture in a JGP450 RF magnetron sputtering system with the process parameters: 200 W of sputtering power, 0.25 Pa of sputtering pressure, and 610 °C of the substrate temperature. The Ar gas flow rate was fixed at 16 ml/min and the oxygen flow rate was fixed at 3.2 ml/min, i.e., the O_2/Ar flow ratio of 0.2:1 was used as working atmosphere. The distance between the substrates and the targets was 11 cm, the sputtering time was 180 min, and the base pressure of the chamber was 1.0×10^{-3} Pa. As-deposited films were annealed in flowing oxygen (99.999%) at 1150 °C for 30 min in a tube furnace.

A Rigaku D/max-rB X-ray diffraction (XRD) meter with Cu K_α-line, X-ray photoelectron spectroscope (XPS, ESCALAB 250) with Al and Mg K_α-lines, a Hitachi S-450 scanning electron microscope (SEM), a Park Autoprobe CP atomic force microscope (AFM) and a Hitachi H-8010 transmission electron microscope (TEM) were the equipments employed to characterize the microstructure, components, crystallinity, and surface morphological properties of the ceramic thin films. The cross-sectional morphologies of the thin films were examined by SEM (S-4800) to evaluate the thickness of the thin film.

* Corresponding author. Tel.: +86 531 86282521; fax: +86 531 86282521.
E-mail address: sf751106@sina.com.cn (F. Shi).

0925-8388/$ – see front matter © 2010 Elsevier B.V. All rights reserved.
doi:10.1016/j.jallcom.2010.11.171

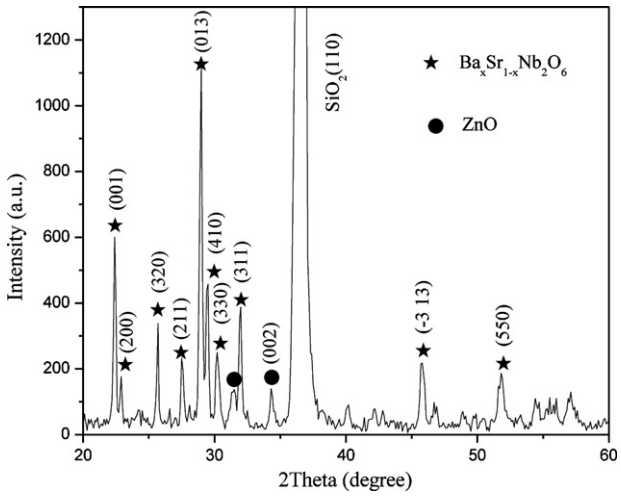

Fig. 1. XRD spectrum of the thin film.

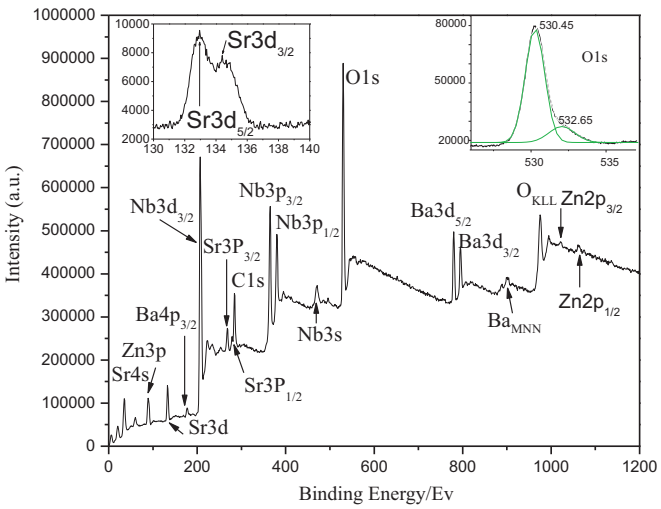

Fig. 2. XPS spectrum of the thin film.

3. Results and discussion

Fig. 1 is the X-ray diffraction patterns of the thin films, exhibiting the presence of the well-crystallized thin films. No preferential orientation for the thin film is observed. The thin films contain a mixture of $Ba_{0.5}Sr_{0.5}Nb_2O_6$ (as compared with the JCPDS card of No. 39-0265, International Center for Diffraction Data, 2002), $Ba_{0.67}Sr_{0.33}Nb_2O_6$ (No. 73-0126), $Sr_{0.744}Ba_{0.247}Nb_2O_6$ (No. 70-3747), and $SrNb_2O_6$ (No. 72-2088), which can be written as $Ba_xSr_{1-x}Nb_2O_6$. And ZnO is also observed, as compared with the characteristic peak of ZnO [9]. As we all know, the various sputtering yields of Ba, Sr, Nb, Zn, and O elements are a knotty problem in the deposition of $(Ba_{0.3}Sr_{0.7})(Zn_{1/3}Nb_{2/3})O_3$-based thin films. The discrepancy between thin film and target probably results from the volatilization of ZnO during the process of sputtering and annealing, because Zn has a significant larger vapor pressure than the other metal elements (Ba, Sr, Nb) [2]. Therefore, ZnO may either not stick to or be re-evaporated from the growing surface [2], worsening the composition deviation with the target.

According to the Scherrer's formula [10], the grain size in the (0 1 3) plane can be estimated by the following expression:

$$L_{(0\,1\,3)} = \frac{\kappa\lambda}{\beta_0 \cos\theta}$$

where κ is a constant with a value of about 0.89 for the Cu target, λ is the X-ray wavelength with a value of about 1.54718 Å, β_0 is the FWHM of the (0 1 3) peak, and θ is the diffraction angle. In the Scherrer's formula, $\beta_0 = 0.003$ rad and $\theta = 29.065^\circ$; therefore, the grain size in the (0 1 3) plane of the thin film is about 52.76 nm.

Fig. 2 shows the XPS spectrum of the thin film in the binding energy range from 0 eV to 1200 eV, and the binding energies at various peaks were calibrated using the C1s (284.6 eV) as a standard sample. The inset images in Fig. 2 show the XPS spectrum of O1s peak. All the XPS spectra of Ba3d, Nb3d, Sr3d, Sr3p, and Zn2p of the thin films consist of two peaks corresponding to their angular momentum of electron. Only one spin–orbit doublet is observed for the individual element, i.e., $Ba3d_{5/2}$ and $Ba3d_{3/2}$ peaks at 780.67 and 795.95 eV, $Nb3d_{5/2}$ and $Nb3d_{3/2}$ peaks at 206.57 and 209.47 eV, $Sr3d_{5/2}$ and $Sr3d_{3/2}$ peaks at 133.07 and 135.02 eV, $Sr3p_{3/2}$ and $Sr3p_{1/2}$ peaks at 267.84 and 278.37 eV, $Zn2p_{3/2}$ and $Zn2p_{1/2}$ peaks at 1023.27 and 1046.51 eV, indicating that only one chemical state exists in the thin films for each element of Ba, Nb, Sr, Zn, i.e., chemical state of Ba^{2+}, Sr^{2+}, Nb^{5+}, and Zn^{2+}. A doublet structure is observed in the XPS spectrum of O1s peak. Its component peak in the spectrum is fitted to a Gaussian-type distribution with the lower binding energy of 530.45 eV and the higher binding energy of 532.65 eV, as shown in the inset spectrum, corresponding to the lattice oxygen and the adsorbed oxygen [10], respectively. In general, the peak of adsorptional oxygen is much weaker than that of lattice oxygen, which would be favorable for the dielectric property of the thin films, because the oxygen vacancies result in the dielectric loss [11]. The quantitative analysis using Ba3d, Sr3d, Zn2p, Nb3d, and O1s peaks reveals that the Ba:Sr:Zn:Nb:O atomic ratio is 3.01:5.33:0.96:27.90:62.80, respectively.

Fig. 3 shows the SEM image of the thin film, which shows that fine spherical particles are distributed on the sample's surface. The surface morphology of the thin film is of dense structure with less small holes. It is evident that the grains are of uniform grain size, and are distributed homogenously on the surface of the thin film.

Fig. 4 shows the thickness of the thin film is about 1.38 μm with dense structure and homogeneous grains and well-defined grain boundaries, which are consistent with the results shown in Fig. 3.

Fig. 5 shows the AFM images of the sample, with a scan area of 10 μm × 10 μm. As seen in Fig. 5(a), the sample is regular in

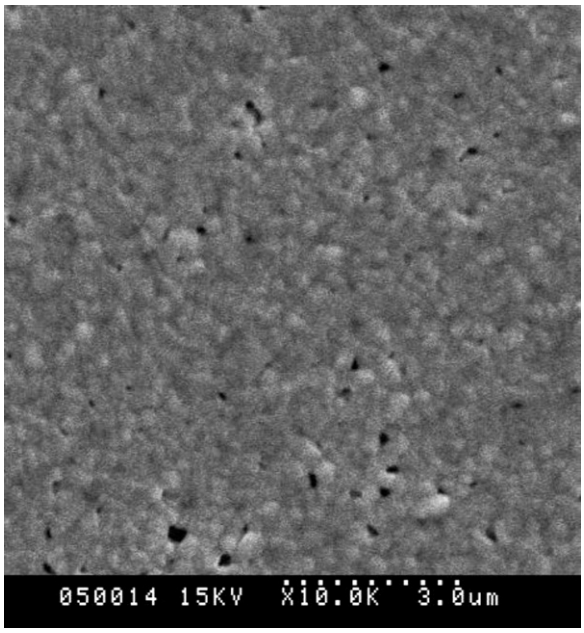

Fig. 3. SEM image of the thin film.

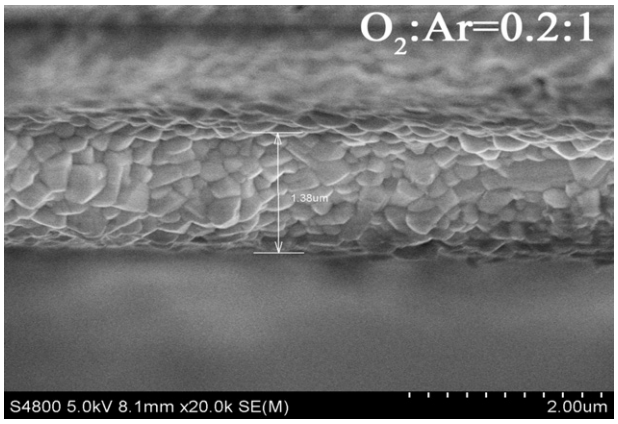

Fig. 4. Cross-sectional SEM images of the thin film.

surface with fine and uniform grains, and a few spherical particles are observed growing along the c axis. The root-mean-square surface roughness (RMS, calculated from the AFM data using the PSI ProScan Image Processing software package version 1.0, Park Scientific Instruments, Sunnyvale, CA) of the thin films is about 27.4 nm. Fig. 5(b) shows the formation of the ceramic thin film with high-quality crystalline.

The TEM image and the selected area electron diffraction (SAED) spectrum are shown in Fig. 6. The spherical particles with the well-defined boundaries are observed in Fig. 6(a). The spherical shape of the grains is consistent with the results acquired by the SEM

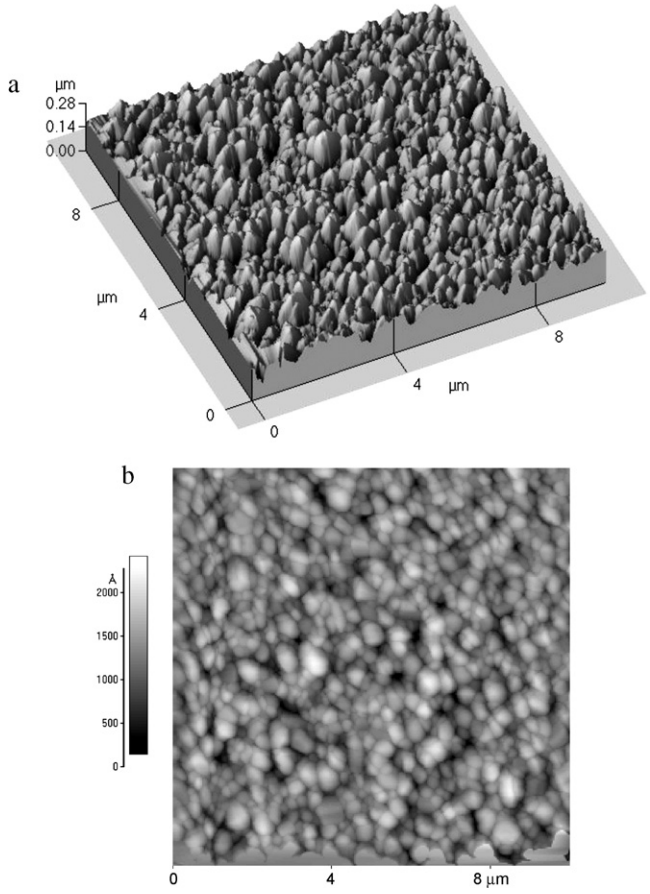

Fig. 5. AFM images of the thin film. (a) Longitudinal cross-section and (b) horizontal cross-section.

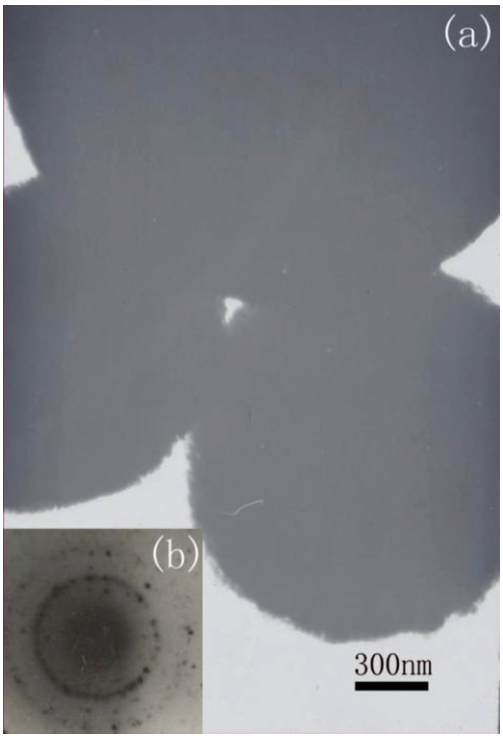

Fig. 6. TEM image and the SAED spectrum of the thin film. (a) TEM and (b) SAED.

and AFM. The SAED spectrum indicates that the thin films are polycrystalline, as shown in Fig. 6(b). About the (0 1 3) grain size, there is considerable discrepancy between the measured grain size (approximate 1600 nm by TEM) and calculation size (53 nm obtains from the Scherrer's formula), which may be because the grain size obtained through the Scherrer's formula is the average size of the orderly arrangement grains, however, the grain size measured by the TEM is the size of the clusters consisting of many small grains, which have not spacial periodicity [12].

4. Conclusion

The main phase of the ceramic thin film is $Ba_xSr_{1-x}Nb_2O_6$. The thin film presents a high crystalline quality, with few adsorbed oxygen. The surface morphology indicates that the thin film is of dense structure. The grains are polycrystalline and uniform in size with the spherical shape and well-defined grain boundaries.

Acknowledgements

The authors would like to thank Associate Professor Xiaokai Zhang for his help in the TEM measurement. The authors are also grateful to Professor Chengshan Xue for his help in discussing our results.

References

[1] M.R. Varma, S. Biju, M.T. Sebastian, J. Eur. Ceram. Soc. 26 (2006) 1903–1907.
[2] Z.Z. Tang, S.J. Liu, R.K. Singh, S. Bandyopadhyay, I. Sus, T. Kotani, M. Schilfgaarde, N. Newman, Acta Mater. 57 (2009) 432–440.
[3] L.N. Gao, J.W. Zhai, X. Yao, Ceram. Int. 34 (2008) 1023–1026.
[4] S.J. Lee, B.Y. Jang, Y.H. Jung, S. Nahm, H.J. Lee, Y.S. Kim, J. Eur. Ceram. Soc. 26 (2006) 2165–2168.
[5] S. Katayama, I. Yoshinaga, N. Yamada, T. Nagai, J. Am. Ceram. Soc. 79 (1996) 2059–2064.
[6] C.W. Cui, F. Shi, Y.G. Li, S.Y. Wang, J. Mater. Sci. - Mater. Electron. 21 (2010) 349–354.

[7] F. Shi, C.W. Cui, Appl. Surf. Sci. 256 (2010) 2626–2670.
[8] A. Ianculescu, B. Despax, V. Bley, T. Lebey, R. Gavrilă, N. Drăgan, J. Eur. Ceram. Soc. 27 (2007) 1129–1135.
[9] Z.M. Yu, S.P. Wu, Q.P. Wei, S.C. Niu, C.C. Peng, J.Z. Li, M. Wei, Vacuum 43 (2006) 11–16.
[10] X. Zhao, Q.H. Yang, J.J. Cui, J. Rare Earths 26 (2008) 511–515 (in Chinese).
[11] C.M. Lu, Q.C. Sun, L. Sun, M.X. Xu, Bull. Chin. Ceram. Soc. 1 (2005) 33–37 (in Chinese).
[12] H. Zhang, Y.S. Liu, W.H. Liu, B.Y. Wang, L. Wei, Acta Phys. Sin. - Chin. Ed. 56 (2007) 7255–7260 (in Chinese).